Orbital Angular Momentum Multiplexing and Demultiplexing by a Single Metasurface

Yang Li, Xiong Li, Lianwei Chen, Mingbo Pu, Jinjin Jin, Minghui Hong, and Xiangang Luo**

Orbital angular momentum (OAM) has recently gained much interest in high-speed optical communication due to its spatial orthogonality. However, complex spatial phase distributions of OAM make the components difficult for nano-photonic integration. In this work, a method to multiplex and demultiplex multiple OAMs, wavelengths, and polarizations channels by a highly integrated off-axis technique on a metasurface is presented. As a multiplexer, beams without OAM can be transferred into coaxial beams carrying different OAM features by different incident angles; as a demultiplexer, coaxial beams carrying multi-OAMs can be divided into different directions with fundamental modes. Furthermore, the component based on dipole optical antenna metasurface can be used not only as an OAM multiplexer/demultiplexer but also as a multiplexer/demultiplexer to achieve wavelength division multiplexing and polarization-division multiplexing, as both these applications are based on the conservations of momentum and angular momentum. For practical applications, phase-only hologram is analyzed to demonstrate multiple functions of this method.

1. Introduction

Orbital angular momentum (OAM) was first discovered in the 1990s, which can be described by a phase cross section of $\exp(il\theta)$, where topological charge l can take unbounded integers.[1–3] Different from spin angular momentum (SAM, also known as circular polarization) that carries information of electric field direction and is limited by the dimensions of space, OAM carries information on the phase distribution of electric field and is unlimited. Due to this unique property, OAM has great potentials in high-speed optical communications. It can be used to add an extra dimension to create an additional set of data carriers for space-division multiplexing (SDM) beyond traditional wavelength-division multiplexing (WDM) and polarization-division multiplexing (PDM).[3,4] Such high-speed communications, which can reach the speed of Tbit s^{-1}, are achieved over both free-space and special vortex fiber using OAM beams multiplexing, WDM and PDM together.[5–7]

High-speed OAM multiplexing communication system, similar to other optical multiplexing communication systems, involves multiplexers and demultiplexers. Traditional OAM multiplexer and demultiplexer consist of OAM generators, such as spatial phase plates (SPPs) or *l*-forked holograms, and channel combiners, for example, cascaded beam splitters.[3–11] The numbers of OAM generators and combiners correspond to the number of channels with independent information uploading by modulators. Therefore, the system becomes complex and less integrated. Several years ago, a method was proposed to solve such complex sequence of holograms and realized multi-OAMs generation and sorting by coordinate transformation.[2] However, this method introduced new challenges. The integration is limited by the distance between two phase plates and the diffraction of light regardless of the thickness of the components used. To make things worse, typical high-speed optical communications, combining not only SDM but also WDM and PDM, require more than one demultiplexer, which further increases the system complexity.

In this paper, we report a physical methodology for multiple OAMs multiplexing and demultiplexing by an off-axis designing principle to integrate all the SDM, WDM, and PDM components into one single ultrathin metasurface. With off-axis incidence of beams representing independent information channels, the component can generate independent coaxial vortex beams with different topological charges as a multiplexer. With vortex beams carrying different OAMs, the channels can be separated into fundamental mode beams at the diverse directions as a demultiplexer. Furthermore, the conservations of momentum make this off-axis diffractive component contain dispersion, which demonstrates its great potentials in SDM-WDM system. For the metasurface based on dipole antenna, there are interesting responses to polarization and OAM, which can be used in PDM-WDM system owing to conservations of momentum and angular momentum. Due to these superior properties, designed metasurface demultiplexer has great potential in high integration of SDM, WDM, and

Dr. Y. Li, Prof. X. Li, Prof. M. Pu, Dr. J. Jin, Prof. X. Luo
State Key Laboratory of Optical Technologies on Nano-Fabrication and Micro-Engineering
Institute of Optics and Electronics
Chinese Academy of Sciences
Chengdu 610209, China
E-mail: lxg@ioe.ac.cn
Dr. Y. Li, Dr. L. Chen, Prof. M. Hong
Department of Electrical and Computer Engineering
National University of Singapore
Engineering Drive 3, Singapore 117576, Singapore
E-mail: elehmh@nus.edu.sg
Dr. Y. Li, Dr. J. Jin
University of Chinese Academy of Sciences
Beijing 100049, China

DOI: 10.1002/adom.201600502

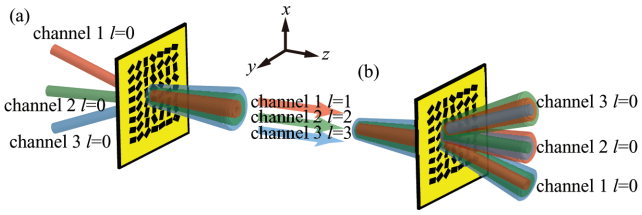

Figure 1. Schematics of a) off-axis incidence multi-OAM multiplexer and b) off-axis multi-OAM demultiplexer.

PDM. Furthermore, phase-only hologram is simulated to prove the multiple functions of our component.

2. OAM Multiplexing and Demultiplexing

OAM multiplexing is to merge multiple channels carrying independent information into coaxial beams with separable OAM topological charges, as shown in **Figure 1**a. Khonina et al. suggested a pioneering method to generate Laguerre–Gauss modes with different indices in prescribed diffraction orders by complex amplitude transmission function superposition.[12] As widely known, OAM is commonly described in Laguerre–Gauss modes. Therefore, it is possible to generate OAM beams with arbitrary topological charges at designed separable directions at a single component. The optical transmission function of this multi-OAM generation via off-axis integration (MOG-OAI) component can be expressed as $t(r,\theta)=\sum_m A_m\ (r)e^{j(l\theta_m+k_{xm}x+k_{ym}y)}$, where k_{xm} and k_{ym} represent the transverse wave vector of the mth channel on x and y-axes, respectively. $A(r)$ dominates the spatial intensity of the beam. r and θ refer to the radial position and the azimuthal coordinate, respectively. Due to the commutativity of k-spaces before and after the multiplexer, directions of independent OAM beams carrying different topological charges can be adjusted by modifying the k-space of incidence. With an off-axis beam incidence, $E_i=e^{k_{x0}x+k_{y0}y}$, the diffraction field at the Fourier plane, which can be designed by integrating a lens, or monitoring the far field, as Fraunhofer diffraction is given by

$$E_F=F\{E_i\cdot t\}=\sum_m F\left\{E_{OAM(l_m)}\left(k_{x0}+k_{xm},k_{y0}+k_{ym}\right)\right\} \quad (1)$$

With a plane wave illuminating the MOG-OAI component at the direction ($-k_{xm}$, $-k_{ym}$) a vortex beam with topological charge l_m can be generated at the direction normal to the component. Therefore, beams carrying independent information are multiplexed together in coaxial beams with separable OAMs by different incident angles. It also works for Gaussian beam incidence as discussed in detail in the Supporting Information.

Figure 1b shows a scheme of OAM channels' demultiplexing. When a beam carrying OAM l_0, $E_i=E_0(r)\cdot e^{jl_0\theta}$, normally illuminates the MOG-OAI component, the Fraunhofer diffraction field can be expressed as $E_F=\sum_m F\left\{E_{OAM(l_m+l_0)}\left(k_{xm},k_{ym}\right)\right\}$.[13] The topological charge of output OAM is the sum of topological charges of incident beam l_0 and an additional OAM l_m modulated by the component. Similar to traditional OAM channel separation, which uses conjugate holograms (or SPPs) to reduce the OAM beams to Gaussian beams, this designed demultiplexer is able to transform the $l=l_0$ beam to $l=0$ at the direction of designed channel $l_m=-l_0$ generation. Therefore, a beam with multi-OAM channels can be demultiplexed to fundamental modes, which can be collected by single-mode waveguides[4] at different directions.

In a SDM communication system, the channel capacity of MOG-OAI component is limited by the space. Rigorously, the capacity is limited by the k-space. The far-field radiation angle θ_l of Laguerre–Gaussian (LG) beam with radial index $p=0$ is $\tan\theta=\sqrt{\frac{|l|}{2}}\frac{\lambda}{\pi w_0}$, where w_0 is the beam waist. The maximum k-space, which is controlled by phase modulation unit, is $1/L$, where L is the lattice constant of the optical modulation unit. The maximum number of OAM channels of the component using off-axis method l_{max} can be estimated as $l_{max}\approx\sqrt[3]{\frac{\pi^2W^2}{L^2}}$ where W is the length/width of the component. Hence, available OAM channels can be increased by enlarging the size of the sample or reducing the size of unit cell.

3. Integration of SDM, WDM, and PDM by a Metasurface

Furthermore, the capacity of an optical system depends on multiple multiplexing methods, instead of a single OAM multiplexing technique. As previous experiments demonstrated methods of OAM applied in high speed communication,[5–7] WDM and PDM are also used to expend the channels. For device miniaturization, SDM, WDM, and PDM techniques should be integrated together, which makes it a great challenge. Fortunately, metasurface, a kind of novel, ultrathin, and integrable optical component, responds to both wavelength and polarization.[14–21] Such kind of metasurface is applied into functional components, such as dispersion elements and polarization splitters.[16,17] Especially, dipole antenna, a kind of metasurface, has broadband dispersionless phase shift ability and different responses to polarizations.[16] Additionally, owing to the off-axis method, the wavelength and polarization information can be transformed to spatial information which can be collected easily. Most recently, Maguid et al. demonstrate the shared-aperture antenna array to realize the OAM measurement with spectrum and polarization of light by reflective metasurface.[22] Therefore, it is possible to integrate SDM, WDM, and PDM together by a single MOG-OAI metasurface.

WDM is one of the most widely used techniques to magnify information capacity in optical communications by uploading the independent signals on channels with different wavelengths. In tradition, beams with different wavelengths can be selected by a spectrometer, which relies on a dispersive element (e.g., blazed grating). For a phase-dispersionless light deflection component, the transverse spatial vector is a constant: $k_x=k\sin(\delta_x)=\frac{2\pi}{\lambda}\sin(\delta_x)=\text{Const.}$, where δ_x is the deflection angle when light passes through the component, which has positive correlation with the wavelength λ. Such kind of spatial separation of different wavelengths is widely used in spectrometers and WDM systems. In an off-axis integrated component, it also works due to the principle of

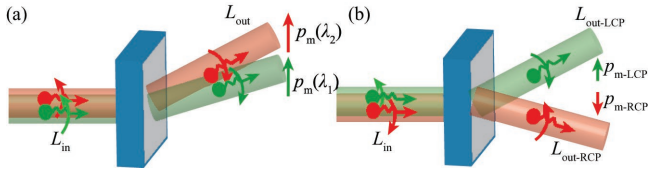

Figure 2. Schematics of conservations in off-axis multi-OAM metasurface. a) Momentum conservation at light illumination of different wavelengths. With the same incident OAM $L_{in} = l_0\hbar$, the output beams have the same OAM $L_{out} = (l_0 + l_m)\hbar$ with the same transverse momentum $p_m(\lambda_1) = p_m(\lambda_2)$. b) Momentum and angular momentum conservations of a component composed by element with opposite phase responses for different polarizations. With a linear polarized light incidence, including both LCP and RCP, the incident OAMs $L_{in} = l_0\hbar$ are transferred to two different OAM beams, $L_{out\text{-}LCP} = (l_0 + l_m)\hbar$ and $L_{out\text{-}RCP} = (l_0 - l_m)\hbar$. The output beams carry opposite transverse momentum $p_{m\text{-}LCP} = -p_{m\text{-}RCP} = k_m\hbar$. However, the sum of momentum and angular momentum does not change.

independent propagation of light. The dispersion follows: $k_{xm} = k_0 \sin(\delta_{xm}) = \frac{2\pi}{\lambda}\sin(\delta_{xm}) = \frac{2\pi}{\lambda_0}\sin(\delta_{xm0})$, where δ_{xm} is the deflection angle of the mth beam. Simultaneously, the dispersionless phase shift ensures unchanged performance in OAM modulation. Therefore, OAM beams with multi-wavelength can be separated without influencing the OAM demultiplexing function.

The chromatism follows the conservations of physical quantities. As shown in **Figure 2**a, the dispersion of the component is due to momentum conservation that $p_m(\lambda)$ is a constant. The photons at different wavelengths have different momentums $p(\lambda) = \frac{2\pi}{\lambda}\hbar$, but the transverse momentums generated by metasurface are unchanged, which is defined by the spatial frequency of the component. For beams with different wavelengths, the propagation directions must be different to maintain the conservation of momentum, which is the dispersion of the component.

PDM is a technique to double the information capacity by polarizations. For optical antennas working on geometric phase, the phase shifts are opposite for the orthogonal incident circular polarizations,[23] such as left-hand and right-hand circular polarizations (LCP and RCP) for dipole antenna[16] and dielectric antenna.[17] Due to this specific property, the MOG-OAI components based on the cross-polarized metasurface have opposite responses to polarization. The diffraction field for LCP and RCP incident light can be expressed as

$$E_{LCP} = F\{E_i \cdot t\} = \sum_m F\left\{E_{OAM(l_m + l_0)}(k_{xm}, k_{ym})\right\} \quad (2)$$

$$E_{RCP} = F\left\{E_i \cdot t^*\right\} = \sum_m F\left\{E_{OAM(-l_m + l_0)}(-k_{xm}, -k_{ym})\right\} \quad (3)$$

The LCP and RCP beams propagate at the opposite directions and get the opposite additional topological charges through the component as well. It means that LCP and RCP beams can be separated into the opposite directions. The RCP beam carrying $l = l_m$ becomes a $l = 0$ beam at the opposite direction for $l = l_m$ generation with LCP incidence. With proper arrangement, the polarization can be separated without affecting the function of OAM demultiplexing. Therefore, it can be utilized as an OAM-PDM demultiplexer. This special response to polarization is caused by the symmetry of space. The symmetry of phase shift leads to conservations of both momentum and angular momentum of photons as shown in Figure 2b. The additional momentums for LCP and RCP must be opposite due to the central symmetry, which leads to opposite deflections; the sum of angular momentums for the LCP and RCP photons does not change after the interaction with the component. Therefore, one $L_{out\text{-}LCP}/L_{out\text{-}RCP}$ increases while another $L_{out\text{-}RCP}/L_{out\text{-}LCP}$ decreases.

4. Simulated Results

In real applications, the functional metasurfaces are designed based on phase-only optical antennas.[16,17,24–29] Especially, the amplitude modulation of the dipole antennas[16,26–28] with the same size is ignorable at different orientations for cross-circular polarized light in the designing processes for applications such as focusing,[28] OAM generation,[16,26] and computer-generated hologram (CGH).[27] In addition, the dispersionless modulation is required. For multiplexing/demultiplexing OAM beams at different wavelengths. The dispersion of amplitude modulation in optical antenna is not as controllable as geometric phase. The amplitude modulation may not match our designed complex amplitude modulation at different wavelengths. Therefore, the phase-only metasurface is designed for simulation. The phase distribution of phase-only component can be expressed as $\varphi_{total}(r,\theta) = \text{Angle}(t)$. Phase-only component losses some amplitude information, which reduces the quality of OAM beams. Nevertheless, most information is reserved. For example, a multiplexer/demultiplexer generating the OAMs $l = -2, -1, 0, 1$, and 2 is designed for a LCP incidence ($\lambda = 632.8$ nm) dipole antenna metasurface. The radius of the component is set as 25 μm; the deflection angle is 9°; the size of pixel is 0.5 μm. **Figure 3**a shows the diffraction image of designed component illuminated by a plane wave. The beams carrying different OAMs propagate at separated directions as predicted in Equation (1). By off-axis illumination at the opposite designed deflection angles, the OAM beams can be combined to coaxial beams with different topological charges as shown in Figure 3b. The intensity and phase distributions are different, but the directions are all normal to the metasurface, which demonstrates its multiplexing function. As an OAM demulitplexer, the fundamental modes appear at the opposite directions for different input OAM beams as shown in **Figure 4**a–c. Figure 4d–f indicates the simulated performance of the dipole antenna metasurface at another incident polarization (RCP). As shown in Figure 4d, the beams propagate at opposite directions with desired opposite OAM. Comparing Figure 4e with Figure 4b, with beams carrying OAM $l = 1$ normal incidence, the diffraction solid spots of LCP and RCP are not directly at the opposite positions. The RCP incident $l = 1$ beam is deflected into the position opposite to LCP $l = 1$ generation as theory predicted in Equations (2) and (3). Therefore, the OAM beams carrying the same topological charges with different polarizations can be separated by the same component for OAM demultiplexing. Beyond polarization response, Figure 4g–i shows demultiplexing of OAM beams at

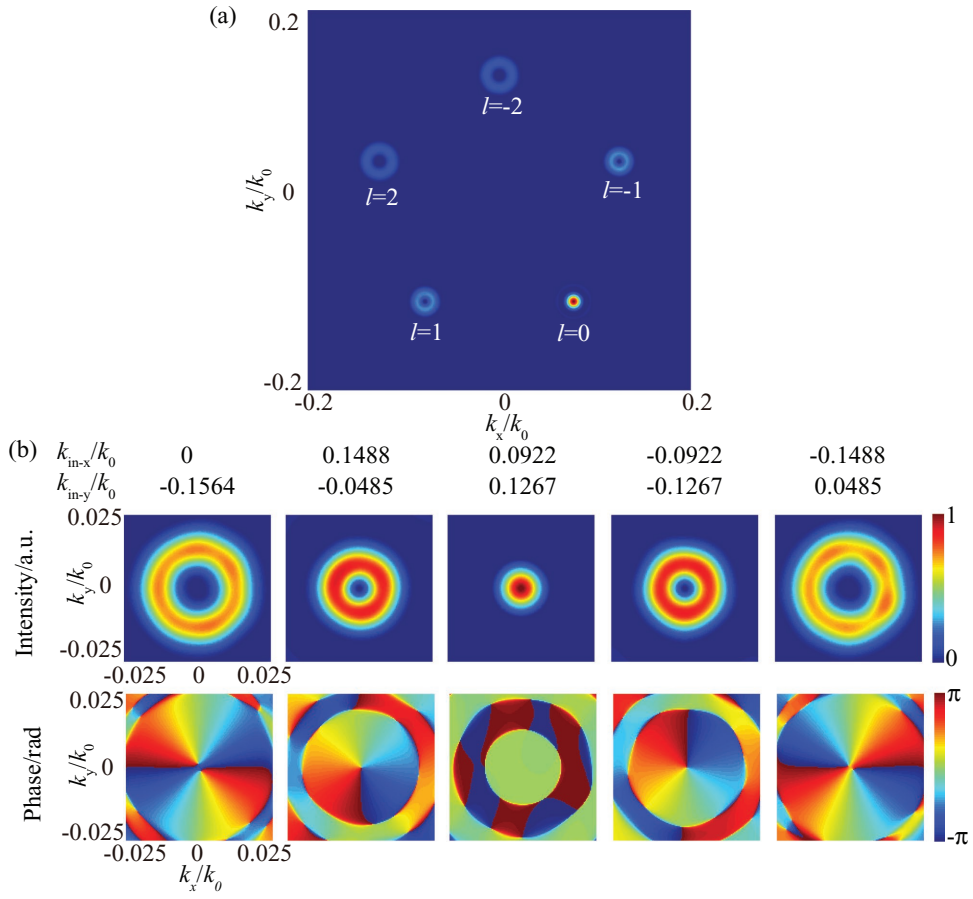

Figure 3. Simulated performance of designed OAM multiplexer. a) Intensity of diffraction image of component illuminated by a normal incidence plane wave ($\lambda = 532$ nm). b) Intensity and phase of the normal output vortex beams carrying different topological charges via off-axis illumination as the deflection angles list in figure.

different wavelengths of 405 (blue), 532 (green), and 632.8 nm (red). The beams with different OAMs are demultiplexed into diverse directions with solid spots, while the beams with the same OAM can propagate at the same direction with diverse deflection angles for different wavelengths. The separation distances can be raised by enlarging the deflection angles.[30] The polarization difference and wavelength can be designed with prescribed range in *k*-space as simulated. These results are calculated based on angular diffraction theory for a general metasurface with geometric phase modulation. A specific metasurface based on nano-slit optical antenna is also simulated by numerical simulation software CST. The results also show the functions of metasurface as theoretically predicted. The detailed results and discussion can be found in the Supporting Information. Therefore, such metasurface based on dipole antenna can be a highly integrated demultiplexer for SDM, PDM, and WDM. Similarly, multiplexers can also support three multiplexing methods by a single component.

5. Conclusion

In conclusion, the theoretical and numerical analyses demonstrate that a single optical component based on metasurface can integrate multiplexing and demultiplexing of OAM, wavelength, and polarization simultaneously by off-axis method. The multi-OAM beams can be perfectly generated via off-axis similar to the conventional method, including SPPs and forked holograms in theory. Via off-axis technique, the directions of OAM are independent and customizable, which gives great flexibility in OAM optical system design. This method can be applied into quantum OAM communication, which can operate two entangled photons symmetrically. It can be used for multi-channels quantum key distribution.[31] Furthermore, the off-axis deflection of each OAM beams makes its wavelength response similar to blazed grating, which can be applied for WDM in communication systems. By the special phase shift elements, off-axis makes the OAM beams carrying opposite topological charges and polarizations deflect to different directions, which can be applied in PDM system. Therefore, demultiplexing of SDM, WDM, and PDM can be done by a single three in one metasurface in OAM communication systems. In addition, utilizing off-axis technique for optical integration has great potentials in complex optical systems with information on space, wavelength, and polarization. It can be applied to color holograms, coding, functional integration, etc. For applications, the phase-only multiplexer and demultiplexer are also demonstrated by simulation.

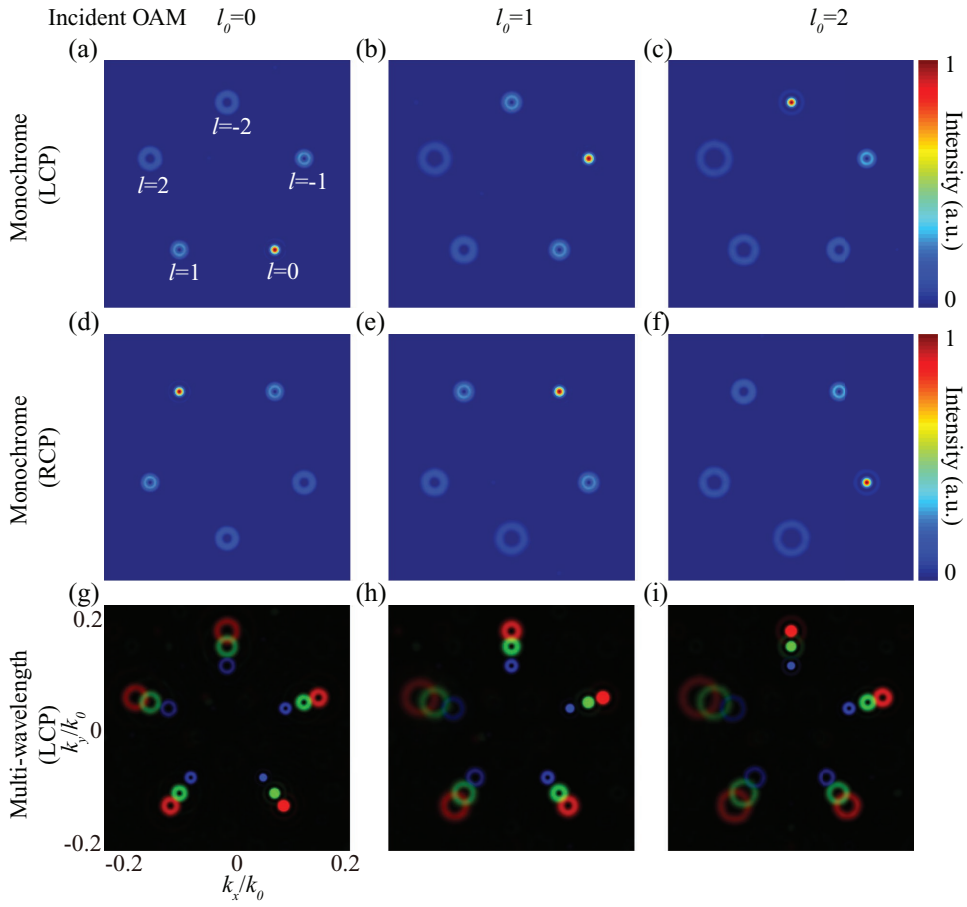

Figure 4. Simulated performance of designed OAM demultiplexer. a–c) The diffraction images of the metasurface illuminated by monochromatic (λ = 532 nm) LCP beams with OAM l_0 = 0, 1, and 2. d–f) The diffraction images of the metasurface illuminated by monochromatic RCP beams with OAM l_0 = 0, 1, and 2. g–i) The diffraction images of the metasurface illuminated by multi-wavelengths (red: λ = 632.8 nm; green: λ = 532 nm; blue: λ = 405 nm) LCP beams with OAM l_0 = 0, 1, and 2.

Supporting Information

Supporting Information is available from the Wiley Online Library or from the author.

Acknowledgements

The authors wish to acknowledge the financial support of National Research Foundation, Prime Minister's Office, Singapore under its Competitive Research Program (CRP Award No. NRF-CRP10-2012-04), 973 Program of China (No. 2013CBA01700), and Chinese Nature Science Grant (Nos. 61138002 and 61622508). L.Y. acknowledges the support from China Scholarship Council (CSC).

Received: June 28, 2016
Revised: September 7, 2016
Published online: November 2, 2016

[1] L. Allen, M. J. Padgett, M. Babiker, *Prog. Opt.* **1999**, *39*, 291.
[2] G. C. G. Berkhout, M. P. J. Lavery, J. Courtial, M. W. Beijersbergen, M. J. Padgett, *Phys. Rev. Lett.* **2010**, *105*, 153601.
[3] A. E. Willner, H. Huang, Y. Yan, Y. Ren, N. Ahmed, G. Xie, C. Bao, L. Li, Y. Cao, Z. Zhao, J. Wang, M. P. J. Lavery, M. Tur, S. Ramachandran, A. F. Molisch, N. Ashrafi, S. Ashrafi, *Adv. Opt. Photonics* **2015**, *7*, 66.
[4] A. M. Yao, M. J. Padgett, *Adv. Opt. Photonics* **2011**, *3*, 161.
[5] H. Huang, G. Xie, Y. Yan, N. Ahmed, Y. Ren, Y. Yue, D. Rogawski, M. J. Willner, B. I. Erkmen, K. M. Birnbaum, S. J. Dolinar, M. P. J. Lavery, M. J. Padgett, M. Tur, A. E. Willner, *Opt. Lett.* **2014**, *39*, 197.
[6] J. Wang, J.-Y. Yang, I. M. Fazal, N. Ahmed, Y. Yan, H. Huang, Y. Ren, Y. Yue, S. Dolinar, M. Tur, A. E. Willner, *Nat. Photonics* **2012**, *6*, 488.
[7] N. Bozinovic, Y. Yue, Y. Ren, M. Tur, P. Kristensen, H. Huang, A. E. Willner, S. Ramachandran, *Science* **2013**, *340*, 1545.
[8] E. Karimi, B. Piccirillo, E. Nagali, L. Marrucci, E. Santamato, *Appl. Phys. Lett.* **2009**, *94*, 231124.
[9] P. Martelli, A. Gatto, P. Boffi, M. Martinelli, *Electron. Lett.* **2011**, *47*, 972.
[10] Y. Yue, Y. Yan, N. Ahmed, J.-Y. Yang, L. Zhang, Y. Ren, H. Huang, K. M. Birnbaum, B. I. Erkmen, S. Dolinar, M. Tur, A. E. Willner, *IEEE Photonics J.* **2012**, *4*, 535.
[11] E. Karimi, S. a Schulz, I. De Leon, H. Qassim, J. Upham, R. W. Boyd, *Light Sci. Appl.* **2014**, *3*, e167.
[12] S. N. Khonina, V. V. Kotlyar, R. V. Skidanov, V. A. Soifer, P. Laakkonen, J. Turunen, *Opt. Commun.* **2000**, *175*, 301.
[13] S. Khonina, V. Kotlyar, V. Soifer, P. Pääkkönen, J. Simonen, J. Turunen, *J. Mod. Opt.* **2001**, *48*, 1543.
[14] W. T. Chen, K.-Y. Yang, C.-M. Wang, Y.-W. Huang, G. Sun, I.-D. Chiang, C. Y. Liao, W.-L. Hsu, H. T. Lin, S. Sun, L. Zhou, A. Q. Liu, D. P. Tsai, *Nano Lett.* **2014**, *14*, 225.

[15] Y. W. Huang, W. T. Chen, W. Y. Tsai, P. C. Wu, C. M. Wang, G. Sun, D. P. Tsai, *Nano Lett.* **2015**, *15*, 3122.
[16] L. Huang, X. Chen, H. Mühlenbernd, G. Li, B. Bai, Q. Tan, G. Jin, T. Zentgraf, S. Zhang, *Nano Lett.* **2012**, *12*, 5750.
[17] D. Lin, P. Fan, E. Hasman, M. L. Brongersma, *Science* **2014**, *345*, 298.
[18] X. G. Luo, *Sci. China: Phys., Mech. Astron.* **2015**, *58*, 1.
[19] M. Pu, Z. Zhao, Y. Wang, X. Li, X. Ma, C. Hu, C. Wang, C. Huang, X. Luo, *Sci. Rep.* **2015**, *5*, 9822.
[20] Z. Zhao, M. Pu, H. Gao, J. Jin, X. Li, X. Ma, Y. Wang, P. Gao, X. Luo, *Sci. Rep.* **2015**, *5*, 15781.
[21] M. Pu, X. Li, X. Ma, Y. Wang, Z. Zhao, C. Wang, C. Hu, P. Gao, C. Huang, H. Ren, X. Li, F. Qin, J. Yang, M. Gu, M. Hong, X. Luo, *Sci. Adv.* **2015**, *1*, e1500396.
[22] E. Maguid, I. Yulevich, D. Veksler, V. Kleiner, *Science* **2016**, *352*, 1202.
[23] M. V. Berry, *J. Mod. Opt.* **1987**, *34*, 1401.
[24] G. Zheng, H. Mühlenbernd, M. Kenney, G. Li, T. Zentgraf, S. Zhang, *Nat. Nanotechnol.* **2015**, *10*, 308.
[25] M. Khorasaninejad, W. T. Chen, R. C. Devlin, J. Oh, A. Y. Zhu, F. Capasso, *Science* **2016**, *352*, 1190.
[26] J. Jin, J. Luo, X. Zhang, H. Gao, X. Li, M. Pu, P. Gao, Z. Zhao, X. Luo, *Sci. Rep.* **2016**, *6*, 24286.
[27] X. Zhang, J. Jin, Y. Wang, M. Pu, X. Li, Z. Zhao, P. Gao, C. Wang, X. Luo, *Sci. Rep.* **2016**, *6*, 19856.
[28] D. Tang, C. Wang, Z. Zhao, Y. Wang, M. Pu, X. Li, P. Gao, X. Luo, *Laser Photonics Rev.* **2015**, *9*, 713.
[29] J. Lin, J. P. B. Mueller, Q. Wang, G. Yuan, N. Antoniou, X.-C. Yuan, F. Capasso, *Science* **2013**, *340*, 331.
[30] M. Born, E. Wolf, *Principles of Optics, 7th ed.*, Cambridge University Press, Cambridge, UK **1999**.
[31] J. Leach, J. Barry, J. Romero, J. Anand, M. Y. Alison, S. Franke-Arnold, D. G. Ireland, R. W. Boyd, S. M. Barnett, M. J. Padgett, *Science* **2010**, *329*, 662.